Geosci. Model Dev. Discuss., 7, 6677–6703, 2014
www.geosci-model-dev-discuss.net/7/6677/2014/
doi:10.5194/gmdd-7-6677-2014

Geoscientific
Model Development
Discussions
Open Access

# A spectral nudging method for the ACCESS1.3 atmospheric model

**P. Uhe and M. Thatcher**

CSIRO Oceans and Atmosphere Flagship, 107–121 Station St, Aspendale,
VIC 3195, Australia

Received: 7 August 2014 – Accepted: 19 September 2014 – Published: 8 October 2014

Correspondence to: P. Uhe (peter.uhe@csiro.au)

Published by Copernicus Publications on behalf of the European Geosciences Union.

## Abstract

A convolution based method of spectral nudging of atmospheric fields is developed in the Australian Community Climate and Earth Systems Simulator (ACCESS) version 1.3 which uses the UK Met Office Unified Model version 7.3 as its atmospheric component. The use of convolutions allow flexibility in application to different atmospheric grids. An approximation using one-dimensional convolutions is applied, improving the time taken by the nudging scheme by 10 to 30 times compared with a version using a two-dimensional convolution, without measurably degrading its performance. Care needs to be taken in the order of the convolutions and the frequency of nudging to obtain the best outcome. The spectral nudging scheme is benchmarked against a Newtonian relaxation method, nudging winds and air temperature towards ERA-Interim reanalyses. We find that the convolution approach can produce results that are competitive with Newtonian relaxation in both the effectiveness and efficiency of the scheme, while giving the added flexibility of choosing which length scales to nudge.

## 1 Introduction

Atmospheric modeling is a discipline that has impacts in many fields of scientific study as well as everyday life. For example, numerical weather prediction (Davies et al., 2005; Puri et al., 2013) provides us our daily weather forecasts and simulations of global climate (Taylor et al., 2012) give us forewarning of possible impacts of climate change. Global climate models are powerful tools, but they have limitations due to grid resolution, approximations to atmospheric physical processes (e.g., convection and turbulent mixing), and also because of incomplete or imperfect datasets such as for representing land-use. Furthermore, since the atmosphere is a chaotic system, the simulated synoptic patterns deviate from observations over time. This makes it more difficult to evaluate modeled behavior, since the advection of tracers depends on the synoptic scale atmospheric circulation. In some cases, to reduce biases caused by these issues, it is useful to introduce a correction to align the model more closely with a host model, often an observational product such as the ERA-Interim reanalysis (ERAI; Dee et al., 2011). The process of adjusting dynamical variables of a model towards a host model is commonly known as nudging (Kida et al., 1991; Telford et al., 2008).

Nudging is useful for model development and scientific studies, where a more realistic atmospheric circulation can help determine errors or feedbacks in particular components of the model. Nudging in atmospheric models has been used to reduce the size of transport errors of trace gases for atmospheric chemistry (Telford et al., 2008) and carbon cycle modeling (Koffi et al., 2012), dynamically downscaling to finer resolution (Wang et al., 2004), and generating regional analyses (von Storch et al., 2000). Two popular approaches to nudging in atmospheric models are Newtonian relaxation (Telford et al., 2008) and spectral nudging (Waldron et al., 1996).

This paper describes an efficient method for implementing a convolution based spectral nudging scheme in atmospheric models, which is demonstrated using the Australian Community Climate and Earth System Simulator (ACCESS; Bi et al., 2013; Dix et al., 2013). The spectral nudging scheme can support irregular grids, making the approach applicable to a wide range of other atmospheric models. We have also significantly improved its computational efficiency by approximating the spectral nudging using one-dimensional (1-D) convolutions, and show that this does not degrade the performance. A convolution approach for spectral nudging using a cubic grid has previously been described by Thatcher and McGregor (2009). However this paper differs from the previous work, as the scheme in ACCESS has been designed to exploit the symmetries of the ACCESS latitude-longitude grid. This paper also provides an extended analysis to compare the performance of various configurations of nudging using Newtonian relaxation and spectral nudging.

ACCESS is a numerical model designed to simulate the Earth's weather and climate systems. ACCESS is used for a wide range of applications from climate change scenarios and numerical weather prediction, to targeted scientific studies into areas such as atmospheric chemistry and aerosols, and the carbon cycle. ACCESS is composed of a number of different submodels, of which the atmospheric component is the UK Met Office Unified Model (UM; Davies et al., 2005; The HadGEM2 Development Team, 2011). The version of ACCESS used in this study, ACCESS1.3, includes the Community Atmosphere Biosphere Land Exchange model (CABLE; Kowalczyk et al., 2013) to represent the land surface. ACCESS often includes ocean and sea-ice components, but these components are not used in this study. A full description of ACCESS can be obtained from Bi et al. (2013).

Nudging was originally implemented in the UM at the University of Cambridge (Telford et al., 2008), using a Newtonian relaxation method. This applies a correction to the model at every time step, calculated from the difference between the host model and the UM. The fields that are nudged are the key dynamical variables; $\Theta$ (potential temperature), $U$ (zonal wind) and $V$ (meridional wind).

An alternate approach to Newtonian relaxation is spectral nudging (von Storch et al., 2000; Thatcher and McGregor, 2009; Waldron et al., 1996). The spectral nudging scheme builds upon and expands the already existing Newtonian relaxation nudging code in the UM. It applies a low-pass spectral filter on the correction calculated as for the relaxation nudging, so the correction is only applied to large spatial scales. The spectral filter is applied using a convolution with a two-dimensional (2-D) Gaussian function. A convolution based filter was chosen rather than using a more conventional Discrete Fourier Transform, as it is simple to implement a parallel version within the UM framework and has the potential to be generalized to irregular and limited area grids. It also operates on the physical distance between grid points, which makes it straight forward to apply consistently across the whole globe and does not require special treatment of the poles. Spectral nudging gives the flexibility of being able to nudge the large scale features of the model towards the host, while allowing the small scales to be determined by the model's own physics. Because of this, spectral nudging is particularly useful in regional climate modeling (Denis et al., 2002; Kanamaru and Kanamitsu, 2007; Kida et al., 1991) and dynamical downscaling (Liu et al., 2012). In these cases, the model resolution is finer than the host model, so there is no information to nudge

Title Page
Abstract | Introduction
Conclusions | References
Tables | Figures
◂◂ | ▸▸
◂ | ▸
Back | Close
Full Screen / Esc
Printer-friendly Version
Interactive Discussion

the finest length scales of the model towards, preventing the effective use of relaxation nudging.

The paper is structured as follows: Sect. 2 covers the implementation and configuration of nudging in ACCESS. This includes Sect. 2.1 covering relaxation nudging, then Sect. 2.2 describing the implementation of the spectral filter and the convolution method used to implement it. A 1-D filter that approximates the 2-D filter is described in Sect. 2.3. The 1-D filter gives significant improvements in the speed of calculating the filter and reduces the amount of message passing. The set up of the model used for simulations presented in this document is covered in Sect. 2.4.

The performance of the spectral nudging is analyzed in Sect. 3. This is split up into subsections relating to different indicators of its performance or looking at the behavior from different parameter choices. Section 3.1 compares the nudged model with ERAI. Section 3.2 compares the performance of the 1-D and 2-D spectral filters. Section 3.3 compares a number of different nudging configurations to see how closely they converge towards ERAI, and the effect of varying the spectral filter length scale. Lastly, Sect. 3.4 investigates the effect of varying the period of nudging, comparing its effect on the temporal spectrum and run times.

## 2 Nudging implementation

The process of nudging aims to perturb prognostic variables $\psi_\mathrm{m}$ of a model (e.g., ACCESS) toward the corresponding variable $\psi_\mathrm{h}$ of a host model (e.g., ERAI). The following section relates how nudging is implemented for each of the different methods used in this paper.

### 2.1 Newtonian relaxation

The standard Newtonian relaxation is applied by taking the difference between $\psi_\mathrm{m}$ and $\psi_\mathrm{h}$, $\Delta\psi = \psi_\mathrm{m} - \psi_\mathrm{h}$, and using this to correct the model,

$$\psi_\mathrm{m} \rightarrow \psi_\mathrm{m} - \alpha\Delta\psi. \tag{1}$$

Here $\alpha \in [0,1]$ is a dimensionless constant determining the strength of nudging. $\alpha$ is related to the concept of an $e$ folding time, which is the length of time to reduce the error by $e^{-1}$, where $\alpha < 1$. The $e$ folding time is $\Delta t/\alpha$ where $\Delta t$ is the period of nudging. For example, a 6 h $e$ folding time with nudging applied every half hour corresponds to $\alpha = 1/12$. $\alpha$ has vertical dependence, and is set to zero below 1000 m (i.e., the typical planetary boundary layer height). This helps avoid conflict between the nudging and the atmospheric model, since the behavior of the atmosphere in the boundary layer is strongly influenced by the land-surface, which can be different between the model and its host.

The code used for the relaxation nudging is based on code from Telford et al. (2008) with some modifications. The code was restructured to improve parallelism when spatially interpolating host data and to use the ERAI dataset as the host model instead of other reanalysis products. The ERAI dataset was also set up with horizontal resolution of 1.875° east–west by 1.25° north–south, compared to 3.75° east–west by 2.5° north–south in the reanalyses used by Telford et al. (2008).

### 2.2 Spectral nudging

Spectral nudging extends the Newtonian relaxation method by taking the correction term and applying a spectral (low-pass) filter so that large spatial wavelengths are adjusted while smaller wavelengths are left essentially unperturbed. The method chosen to do this is based on Thatcher and McGregor (2009), using a convolution of $\Delta\psi$ with a Gaussian function, $w$, to implement the filter. However, the approach in this paper differs from previous work in its application to the ACCESS grid, requiring different implementation of the convolution for different underlying grids.

The correction for spectral nudging is applied as follows:

$$\psi_\mathrm{m} \rightarrow \psi_\mathrm{m} - \alpha(\Delta\psi * w) \tag{2}$$

where $*$ is the convolution operator. The convolution is calculated on the surface of a sphere (assumed to have radius $R = 1$). This results in:

$$\Delta\psi * w = \iint \Delta\psi(\theta', \phi') w(\theta' - \theta, \phi' - \phi) \cos(\phi') \mathrm{d}\phi' \mathrm{d}\theta' \tag{3}$$

where the Gaussian weighting function is:

$$w(\theta' - \theta, \phi' - \phi) = \frac{1}{b} \exp\left(\frac{-\Delta\sigma^2}{2\lambda^2}\right). \tag{4}$$

$\lambda$ is the standard deviation of the Gaussian function, which is referred to as the nudging length scale. $\theta$ and $\phi$ are the azimuthal angle and polar angle respectively, and $\theta'$ and $\phi'$ are dummy co-ordinates that are integrated over. $b$ is a normalization factor, $b = \iint \exp\left(\frac{-\Delta\sigma^2}{2\lambda^2}\right) \mathrm{d}\phi' \mathrm{d}\theta'$. Note that $b$ is evaluated after the expression is discretized. $\Delta\sigma(\theta' - \theta, \phi' - \phi)$ is the distance of a chord between the two points $(\theta', \phi')$ and $(\theta, \phi)$:

$$\Delta\sigma = 2 \arcsin\left(\frac{C}{2}\right) \tag{5}$$

where $C(\theta' - \theta, \phi' - \phi)$ is the Cartesian distance between the points $(\theta', \phi')$ and $(\theta, \phi)$. Combining and discretizing Eqs. (3), (4) and (5), we get the correction that is applied by the scale selective filter.

The ACCESS grid is horizontally decomposed into domains that are assigned to individual processors. The calculation of the convolution at any point requires a global sum. Global information is not stored on individual processors, so the Message Passing Interface (MPI) is used to gather the $\Delta\psi$ arrays handled by each processor into a global array, and broadcast them to all processors. Each processor calculates the convolution just for its domain using this global information.

The naive implementation of the spectral filter involves a large computational effort (of order $N^2$ computations for $N$ horizontal grid points). A spectral filter could be implemented more efficiently via a Fast Fourier Transform (FFT), or a spherical harmonic transform, requiring order $N \log_2 N$ computations, but the convolution gives much greater flexibility to be used with different grid configurations, from the regular latitude-longitude grid to irregular or limited area grids. To mitigate the computational effort of the convolution, a 1-D approximation to the convolution has been developed, described in the following section.

### 2.3 1-D filter

To improve the computational efficiency of the spectral nudging scheme, the 2-D convolution can be separated into two 1-D convolutions, thereby reducing the computational effort to order $N^{3/2}$. The 2-D convolution is separated by splitting the Gaussian function into parts that depend solely on latitude or longitude. The two integrals in the 2-D filter can then be evaluated separately as two 1-D convolutions. The expression for the two 1-D convolutions is equal to the 2-D convolution on a flat Cartesian grid, but is an approximation on a curved surface such as the global latitude-longitude grid.

$$w(\theta'-\theta,\phi'-\phi) \approx \frac{1}{b} w(\theta'-\theta,\phi) w(\theta',\phi'-\phi) \tag{6}$$

$$\approx \frac{1}{b} \exp\left(\frac{-\Delta\sigma(\theta'-\theta,\phi)^2}{2\lambda^2}\right) \exp\left(\frac{-\Delta\sigma(\theta',\phi'-\phi)^2}{2\lambda^2}\right). \tag{7}$$

A 1-D convolution is applied in one direction, then another 1-D convolution is applied on the result of the first convolution.

$$\Delta\psi * w \approx \frac{1}{b}[\Delta\psi * w(\theta', \phi' - \phi)] * w(\theta' - \theta, \phi) \tag{8}$$

$$\approx \frac{1}{b}\int \left[\int w(\theta', \phi' - \phi)\Delta\psi(\theta', \phi')\cos(\phi')\mathrm{d}\phi'\right] w(\theta' - \theta, \phi)\mathrm{d}\theta'. \tag{9}$$

Since the integrals are computed independently, $w$ is calculated along horizontal rows and columns separately, not over the whole globe. Consequently, the code scales better with increasing numbers of processors. As well as computational speedup, this reduces communication bottlenecks from data passed through MPI. Rather than global arrays being broadcast to every processor, each processor only needs data passed from processors associated with the same rows or columns of the horizontal grid.

Using this 1-D approximation, there is a choice in which convolution to apply first (i.e., either the zonal or meridional directions). Swapping the order of the integrals (convolutions) results in numerically different solutions. It is found that to reduce the error it is best to apply the convolution first along the latitudinal direction then longitudinally. This is discussed in Sect. 3.2, which compares the different orderings of the 1-D filter with the 2-D filter.

It also needs to be noted that the 1-D spectral filter is dependent on the model grid and the way the grid is decomposed into domains for each processor. The configuration of the ACCESS grid allows the convolution to be computed along rows of equal latitude or longitude and those results efficiently distributed to rows or columns of processors. This approach needs to be modified for grids which do not have these symmetries. See Thatcher and McGregor (2009) for an example of a 1-D spectral filter applied on a cubic grid.

## 2.4 Model configuration/description

This paper uses simulations of ACCESS, in the ACCESS1.3 atmosphere only configuration (Bi et al., 2013). This uses the atmospheric model UM vn7.3, CABLE 1.8 (Kowalczyk et al., 2013), as well as prescribed sea-surface temperatures and sea-ice concentrations. The model horizontally uses a N96 grid (uniform latitude longitude grid with 1.875° east-west and 1.25° north south resolution). It has 38 vertical levels which are terrain following hybrid height levels, representing heights from 10 m to 36 km. The model was run with a 30 min time step.

A series of one year simulations were run, starting from the 1 January 1990, each initialized in the same state, from a previous climate simulation, i.e. with an initial state unrelated to any historical synoptic patterns. The only differences between simulations were in the nudging configuration. These short experiments were chosen to to evaluate the performance of different nudging methods and choice of nudging parameters. Longer climate simulations may also provide more in depth insight into biases in the nudging scheme, but this evaluation is beyond the scope of this paper.

The nudging component used the ERAI reanalysis product as the host model, provided at 6 hourly intervals. The ERAI data was interpolated onto the ACCESS grid and linearly interpolated temporally to each time step. Nudging was applied above vertical level 7, corresponding to about 1 km in height above the surface terrain. The nudging amplitude $\alpha$, was ramped up from 0 to the full strength over 3 vertical levels so as to reduce the discontinuity between nudged and non-nudged parts of the atmosphere.

The parameters varied in the experiments were the nudging method, nudging period, maximum nudging strength, and spectral filter length. The relaxation nudging is always applied every time step, and the spectral filter can be applied at frequencies that are multiples of the time step and divide into 6 h (e.g. 0.5, 1, 2, 3 or 6 h). Simulations presented use a maximum nudging strength corresponding to either a one hour *e* folding time (referred to as hard nudging) or six hour *e* folding time (referred to as soft nudging). Simulations were run with a range of filter length scales, from 0.03–0.5 radians.

## 3 Results and discussion

To determine the performance of the spectral filter we look at the nudged runs compared with ERAI, as well as comparing with a control simulation without nudging. The analysis was conducted in all cases on the air temperature field, measured on a plane of constant pressure at 500 hPa.

### 3.1 Analysis of mean state and variance in the nudged model

Figure 1 shows the spatial distribution of root mean squared error (RMSE) for different ACCESS simulations, where we are defining the error as the difference between ACCESS and ERAI and calculating it over one year of simulation, for the 6 hourly intervals the ERAI data is provided on. For these plots, a control simulation with no nudging is compared against simulations using relaxation nudging and spectral nudging. The 1-D filter was chosen as the preferred method of spectral nudging as discussed further in Sect. 3.2. In all cases, the nudged runs have much smaller error than the control simulation. The spectral filter with small length scales nudged (Fig. 1c) results in behavior similar to the relaxation nudging (Fig. 1b). As the filter length scale is increased, larger wavelengths are able to deviate from ERAI, and the magnitudes of the deviations are larger (Fig. 1d). It is also worthwhile to note the greatest deviations occur over the Himalayas, where there is a mismatch in the orographic height between ACCESS and ERAI.

Figure 2 shows the difference in the variance between the ACCESS simulations and ERAI. The variance in the ACCESS control simulation is consistently higher than ERAI, shown in Fig. 2a. Nudging constrains the variance to much more closely match the variance in ERAI than the control simulation. There is a similar magnitude of difference in the variance for each of the nudging simulations. The nudged simulations have greater variance than ERAI over some land masses, but lower variance over the oceans. Investigation into the reason for this is the subject of future work.

### 3.2 Evaluation of 1-D approximation

The approximation used in the 1-D spectral filter can be tested by comparing the results with simulations using the 2-D filter. There are two ways to order the convolutions in the 1-D filter, with the zonal convolution followed by the meridional convolution (1-D filter, lon-lat), or the meridional convolution followed by the zonal convolution (1-D filter, lat-lon).

The global Root Mean Squared Error (RMSE) is very similar between the different methods of spectral nudging. Simulations using hard nudging and a filter length of $\lambda = 0.1$ applied once an hour, give an RMSE of 0.415 K for the 2-D filter, 0.414 K for the 1-D filter lat-lon and 0.416 K for the 1-D filter lon-lat, in air temperature at 500 hPa, over one year of simulation.

To more closely compare the different ordering of the 1-D convolutions, Fig. 3 shows the RMS difference between simulations using the 1-D filters and the 2-D filter. In polar regions, there is a greater difference between the 2-D filter and the 1-D filter in the lon-lat case, This indicates that the lat-lon case is a better approximation of the 2-D filter than the lon-lat.

The difference between the lon-lat and the lat-lon version of the 1-D filter occurs because the grid points near the pole are physically close together in the longitudinal direction. A small error at the pole could be spread zonally across multiple grid points. In the lon-lat case, this error will remain after the initial zonal convolution. On the other hand, when the meridional convolution is applied first, the error near the poles can be reduced. This is because the values at grid boxes close to the poles have a smaller weighting in the meridional convolution as they have a smaller area.

The other differences between the 1-D and 2-D filter shown in Fig. 3, can be attributed to small numerical differences which grow over time in a chaotic system. These differences are especially noticeable near the equator. However, the time averaged RMSEs relative to ERAI quoted above, show no significant difference between the 1-D and 2-D filters. Hence the 1-D filter gives a different result to the 2-D filter, but constrains the model to a similar extent. Because of this, and the reduction in computational effort compared to the 2-D filter, the 1-D filter with the meridional convolution applied first is taken as the optimum choice. All simulations using spectral nudging refer to this configuration, except where specified otherwise.

### 3.3 Performance of the spectral filter

Figure 4 shows time-series of RMSE of relaxation and spectral nudging simulations, using different filter length scales and *e* folding times. Each spectral nudging simulation uses hourly nudging. The convergence of RMSE depends on the combination of *e* folding time and nudging length scale (for the spectral nudging). The model is more tightly constrained using the shorter *e* folding time (hard nudging) and smaller nudging length scales. The spectral filter with $\lambda = 0.1$ and one hour *e* folding time, gives a RMSE similar to the relaxation nudging with a six hour *e* folding time. The more tightly constrained simulations reach a steady state more quickly, and all the simulations shown have reached a steady RMSE within four days of simulation or less (not visible for the time scale of this plot).

It is also useful to compare the performance of the model between small and large spatial scales. The RMSE gives the error grid point by grid point, at the smallest length scale. To evaluate the error at the largest length scale (the whole globe), the global mean of the difference between ACCESS and ERAI can be used. We refer to this as the Global Average Error (GAE). The GAE tends to drift over time rather than settle down to a constant value, so the values of GAE presented in Table 1 include a 95 % confidence interval as a measure of the uncertainty. Future work will involve conducting multi-year simulations to obtain more conclusive statistics regarding biases or trends in the GAE.

Table 1 shows that the simulations that are more tightly constrained in RMSE do not necessarily result in lower GAE, though we do note that the more tightly constrained simulations have smaller fluctuations in the GAE (not shown). For example, the hard spectral nudging with $\lambda = 0.1$ has a greater RMSE, but smaller GAE than the hard relaxation nudging. The RMSE quantifies how large the magnitude of errors are at each grid box whereas the GAE indicates how much ACCESS is warmer or cooler than ERAI, averaged over the globe. The smaller GAE for the spectral nudging can be explained by the relaxation nudging resulting in smaller errors at each grid box, but a tendency for those errors to be in the same direction (warmer), while the spectral nudging has larger errors at each grid box but with these errors averaging out at the large spatial scales.

To further show the effect of the spectral filter at different length scales, the simulation output was re-gridded to a range of coarser resolutions. Re-gridding to coarser resolutions removes the fine scale detail in a similar way to the spectral filter, so the performance of the spectral filter should improve at coarser resolutions. This is shown by Fig. 5, which compares the RMSE at different re-gridded resolutions for different simulations.

At the highest resolutions, the relaxation nudging has a smaller RMSE, showing that it constrains the small length scales more tightly than the spectral nudging. For the spectral nudging, decreasing $\lambda$ reduces the RMSE at all length scales (i.e. shifts the curve downward). At coarser re-gridded resolutions, the spectral nudging simulations with $\lambda = 0.1$ and $\lambda = 0.2$ have lower RMSE than the relaxation nudging. Hence, the spectral nudging can capture the large scale structures of ERAI better than the relaxation nudging. The spectral nudging with $\lambda = 0.5$ has a greater RMSE for all re-gridded resolutions apart from the largest, indicating that the filter is not as effective at constraining the model in this case. From this we can choose relaxation nudging or spectral nudging with a smaller or greater $\lambda$, depending on which spatial length scales we want to constrain.

### 3.4 Nudging period

Figure 6 shows the temporal spectra from simulations using different nudging configurations. Relaxation nudging is applied every time step, so the nudging period is only applicable to the spectral filter. Nudging can be applied at intervals from every time step (30 min), to the period of the host data (6 h in the case of ERAI).

All valid choices of nudging period are able to sufficiently constrain the model, given a comparable *e* folding time. The choice of nudging therefore, is a trade-off between computational effort and increased nudging shock, as constraining the model when nudging less frequently requires larger adjustments to the perturbed field. Nudging less frequently hence causes distortions to the temporal spectra as shown in Fig. 6. However less frequent nudging offers a significant speedup as discussed below.

Examining Fig. 6 in more detail, it is evident that nudging with a period of six hours results in spikes in the Fourier spectrum at certain frequencies. This shows that the nudging adjustment is unbalancing the atmospheric model, causing it to respond unevenly in the spectrum. When nudging every hour, these imbalances are removed. Apart from a distortion in the spectrum below half an hour (one time step) the line for spectral nudging every hour lies on top on the line for spectral nudging every time step.

The spectra when nudging every time step is qualitatively similar to the control simulation, but shifted down in magnitude. The spectral nudging every time step has a spectrum in between the curves for the control and relaxation nudging. The spectrum for the 2-D filter is indistinguishable to the equivalent simulations using the 1-D spectral filter with the same filter length scale (2-D filter not shown).

Considering the speed benefits of different nudging frequencies, the 1-D spectral filter nudged every 6 h adds 3.3 % to the run time (the same as Newtonian relaxation). When the period is decreased to 1 h or 30 min this increases the run time by 6.7 and 12 % respectively. The 2-D spectral filter in comparison adds 33 % when nudged every 6 h, increasing to 190 and 376 %, which is not viable for most uses.

Nudging at hourly intervals can be used as a compromise between speed of computation and reducing the distortions in the spectra, and is the standard period of nudging used for spectral nudging in this paper.

## 4 Conclusions

This paper has introduced the use of spectral nudging in the UM and ACCESS. This is achieved through a novel convolution method, first described by Thatcher and McGregor (2009), but generalized in this paper for use with latitude-longitude grids as used by the ACCESS atmospheric model. Analysis of the different configurations of nudging shows that the nudging schemes effectively constrain the nudged fields to follow the host model (ERAI). We have surveyed the spectral filter across a range of filter length scales. The spectral nudging scheme approaches the Newtonian relaxation nudging when small length scales are nudged, but allows the flexibility to nudge only large spatial structures when the filter length scale is increased.

The 1-D spectral filter is shown to perform as well as the 2-D filter, while producing a speedup of 10–30 times. This is achieved by the approximation of separating the 2-D convolution into 1-D convolutions and by using symmetries of the model grid to reduce communication between processors. We also identified that due to the geometry of our grid, the order of convolutions in the 1-D filter was important. To reduce error in the approximation, the meridional convolution is applied first.

Nudging with different frequencies was also investigated, showing that nudging every six hours is still able to constrain the model, but introduces distortions to the spectra. Nudging once an hour produces a speed up in comparison to nudging every time step, while introducing minimal distortions so was used for the majority of simulations.

The approach used to implement the 2-D and 1-D spectral filters is applicable to many other models. The 2-D convolution method can be implemented on any grid, though it suffers from being computationally expensive. The 1-D filter can be applied to irregular or more complex grids, but would require modification to separate the 2-D Gaussian function using an approximation that is appropriate for the particular grid.

Future work on spectral nudging in ACCESS will involve generalizing the spectral nudging to limited area and stretched grid configurations. Another potential approach to gaining a speedup in the convolution based spectral filter is to compute the convolutions over a small neighborhood, rather than the whole globe, ignoring areas where the Gaussian function has values close to zero. The ability to extend the convolution based spectral filter within the ACCESS/UM framework and in other modeling systems is an advantage of this approach.

## Code availability

Due to intellectual property right restrictions, CSIRO cannot publish the full source code for ACCESS or the UM. The Met Office Unified Model (UM) with the spectral nudging source code and configuration described in this paper can be obtained under an end user license agreement (EULA) from CSIRO for educational and non-commercial research use for specific projects. To request a EULA for the modified UM, and/or to obtain the ACCESS1.3 model configuration used in this paper, please contact Tony Hirst (tony.hirst@csiro.au).

*Acknowledgements.* Thanks to Peter Dobrohotoff, John McGregor and Tony Hirst for their feedback. The simulations were conducted on the raijin supercomputing cluster at the NCI (National Computing Infrastructure). This work included funding by the Australian Government through the Australian Climate Change Science Programme. ERA-Interim data, from the European Centre for Medium-Range Weather Forecasts (ECMWF) was used in this research. The UM was made available to CSIRO under the Consortium Agreement: Met Office's Unified Model Earth System Modelling software (Met Office Ref L1587).

# References

Bi, D., Dix, M., Marsland, S., O'Farrell, S., Rashid, H., Uotila, P., Hirst, A., Kowalczyk, E., Golebiewski, M., Sullivan, A., Yan, H., Hannah, N., Franklin, C., Sun, Z., Vohralik, P., Watterson, I., Zhou, X., Fiedler, R., Collier, M., Ma, Y., Noonan, J., Stevens, L., Uhe, P., Zhu, H., Griffies, S., Hill, R., Harris, C., and Puri, K.: The ACCESS coupled model: description, control climate and evaluation, Aust. Met. Oceanogr. J., 63, 41–64, 2013. 6679, 6680, 6686

Davies, T., Cullen, M. J. P., Malcolm, A. J., Mawson, M. H., Staniforth, A., White, A. A., and Wood, N.: A new dynamical core for the Met Office's global and regional modelling of the atmosphere, Q. J. Roy. Meteor. Soc., 131, 1759–1782, doi:10.1256/qj.04.101, 2005. 6678, 6680

Dee, D. P., Uppala, S. M., Simmons, A. J., Berrisford, P., Poli, P., Kobayashi, S., Andrae, U., Balmaseda, M. A., Balsamo, G., Bauer, P., Bechtold, P., Beljaars, A. C. M., van de Berg, L., Bidlot, J., Bormann, N., Delsol, C., Dragani, R., Fuentes, M., Geer, A. J., Haimberger, L., Healy, S. B., Hersbach, H., Hólm, E. V., Isaksen, L., Kållberg, P., Köhler, M., Matricardi, M., McNally, A. P., Monge-Sanz, B. M., Morcrette, J.-J., Park, B.-K., Peubey, C., de Rosnay, P., Tavolato, C., Thépaut, J.-N., and Vitart, F.: The ERA-Interim reanalysis: configuration and performance of the data assimilation system, Q. J. Roy. Meteor. Soc., 137, 553–597, doi:10.1002/qj.828, 2011. 6679

Denis, B., Coté, J., and Laprise, R.: Spectral decomposition of two-dimensional atmospheric fields on limited-area domains using the discrete cosine transform (DCT), Mon. Weather Rev., 130, 1812–1829, 2002. 6680

Dix, M., Vohralik, P., Bi, D., Rashid, H., Marsland, S., O'Farrell, S., Uotila, P., Hirst, T., Kowalczyk, E., Sullivan, A., Yan, H., Franklin, C., Sun, Z., Watterson, I., Collier, M., Noonan, J., Rotstayn, L., Stevens, L., Uhe, P., and Puri, K.: The ACCESS couple model: documentation of core CMIP5 simulations and initial results, Aust. Met. Oceanogr. J., 63, 83–99, 2013. 6679

Kanamaru, H. and Kanamitsu, M.: Scale-selective bias correction in a downscaling of global analysis using a regional model, Mon. Weather Rev., 135, 334–350, 2007. 6680

Kida, H., Koide, T., Sasaki, H., and Chiba, M.: A new approach for coupling a limited area model to a GCM for regional climate simulations, J. Meteorol. Soc. Jpn., 69, 723–728, 1991. 6679, 6680

Koffi, E. N., Rayner, P. J., Scholze, M., and Beer, C.: Atmospheric constraints on gross primary productivity and net ecosystem productivity: results from a carbon-cycle data assimilation system, Global Biogeochem. Cy., 26, 1–15, doi:10.1029/2010GB003900, 2012. 6679

Kowalczyk, E., Stevens, L., Law, R., Dix, M., Wang, Y., Harman, I., Haynes, K., Srbinovsky, J., Pak, B., and Ziehn, T.: The land surface model component of ACCESS: description and impact on the simulated surface climatology, Aust. Met. Oceanogr. J., 63, 65–82, 2013. 6680, 6686

Liu, P., Tsimpidi, A. P., Hu, Y., Stone, B., Russell, A. G., and Nenes, A.: Differences between downscaling with spectral and grid nudging using WRF, Atmos. Chem. Phys., 12, 3601–3610, doi:10.5194/acp-12-3601-2012, 2012. 6680

Puri, K., Dietachmayer, G., Steinle, P., Dix, M., Rikus, L., Logan, L., Naughton, M., Tingwell, C., Xiao, Y., Barras, V., Bermous, I., Bowen, R., Deschamps, L., Franklin, C., Fraser, J., Glowacki, T., Harris, B., Lee, J., Le, T., Roff, G., Sulaiman, A., Sims, H., Sun, X., Sun, Z., Zhu, H., Chattopadhyay, M., and Engel, C.: Implementation of the initial ACCESS numerical weather prediction system, Aust. Met. Oceanogr. J., 63, 265–284, 2013. 6678

Taylor, K., Stouffer, R. L., and Meehl, G. A.: An Overview of CMIP5 and the experiment design, B. Am. Meteorol. Soc., 93, 485–498, doi:10.1175/BAMS-D-11-00094.1, 2012. 6678

Telford, P. J., Braesicke, P., Morgenstern, O., and Pyle, J. A.: Technical Note: Description and assessment of a nudged version of the new dynamics Unified Model, Atmos. Chem. Phys., 8, 1701–1712, doi:10.5194/acp-8-1701-2008, 2008. 6679, 6680, 6682

Thatcher, M. and McGregor, J. L.: Using a scale-selective filter for dynamical downscaling with the conformal cubic atmospheric model, Mon. Weather Rev., 137, 1742–1752, doi:10.1175/2008MWR2599.1, 2009. 6679, 6680, 6682, 6685

The HadGEM2 Development Team: G. M. Martin, Bellouin, N., Collins, W. J., Culverwell, I. D., Halloran, P. R., Hardiman, S. C., Hinton, T. J., Jones, C. D., McDonald, R. E., McLaren, A. J., O'Connor, F. M., Roberts, M. J., Rodriguez, J. M., Woodward, S., Best, M. J., Brooks, M. E., Brown, A. R., Butchart, N., Dearden, C., Derbyshire, S. H., Dharssi, I., Doutriaux-Boucher, M., Edwards, J. M., Falloon, P. D., Gedney, N., Gray, L. J., Hewitt, H. T., Hobson, M., Huddleston, M. R., Hughes, J., Ineson, S., Ingram, W. J., James, P. M., Johns, T. C., Johnson, C. E., Jones, A., Jones, C. P., Joshi, M. M., Keen, A. B., Liddicoat, S., Lock, A. P., Maidens, A. V., Manners, J. C., Milton, S. F., Rae, J. G. L., Ridley, J. K., Sellar, A., Senior, C. A., Totterdell, I. J., Verhoef, A., Vidale, P. L., and Wiltshire, A.: The HadGEM2 family of Met Office Unified Model climate configurations, Geosci. Model Dev., 4, 723–757, doi:10.5194/gmd-4-723-2011, 2011. 6680

von Storch, H., Langenberg, H., and Feser, F.: A spectral nudging technique for dynamical downscaling purposes, Mon. Weather Rev., 128, 3664–3673, 2000. 6679, 6680

Waldron, K., Paegle, J., and Horel, J.: Sensitivity of a spectrally filtered and nudged limited-area model to outer model options, Mon. Weather Rev., 124, 529–547, 1996. 6679, 6680

Wang, Y., Leung, L. R., McGregor, J. L., Lee, D.-K., Wang, W.-C., Ding, Y., and Kimura, F.: Regional climate modelling: progress, challenges and prospects, J. Meteorol. Soc. Jpn., 82, 1599–1628, 2004. 6679

**Table 1.** Comparison of RMSE and GAE in air temperature at 500 hPa measured in Kelvin, for one year of simulation, using different nudging methods. Spectral nudging experiments use nudging applied once an hour. Uncertainty quoted for GAE is based on a 95 % confidence interval

| Experiment | RMSE | GAE |
|---|---|---|
| Relaxation, soft | 0.39 | 0.03 ± 0.02 |
| Spectral, soft, $\lambda = 0.1$ | 0.65 | −0.05 ± 0.03 |
| Relaxation, hard | 0.26 | 0.07 ± 0.01 |
| Spectral, hard, $\lambda = 0.03$ | 0.29 | 0.05 ± 0.01 |
| Spectral, hard, $\lambda = 0.1$ | 0.41 | −0.002 ± 0.02 |
| Spectral, hard, $\lambda = 0.2$ | 0.83 | −0.02 ± 0.05 |

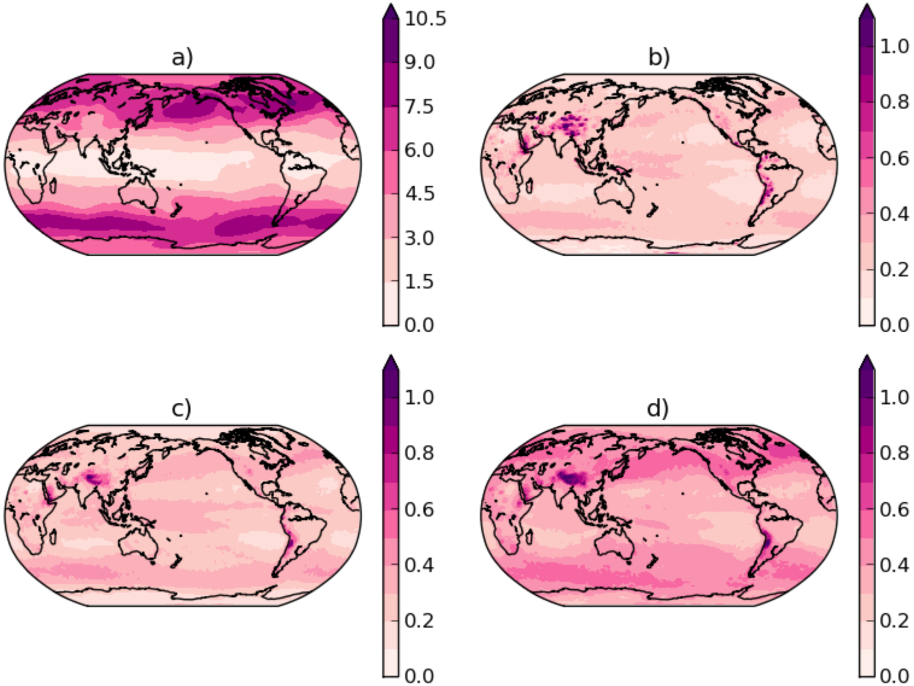

**Figure 1.** Spatial distributions of the RMSE in air temperature of ACCESS simulations. This is measured in Kelvin on a 2-D horizontal plane at 500 hPa and averaged over one year of simulation. **(a)** is the control with no nudging. **(b)** is the relaxation nudging with hard nudging. **(c** and **d)** are spectral nudging using the 1-D filter with hard nudging, applied once an hour. Different nudging length scales were used: $\lambda = 0.1$ in **(c)** and $\lambda = 0.2$ in **(d)**. Note, for clarity, **(a)** uses a different scale for the contours.

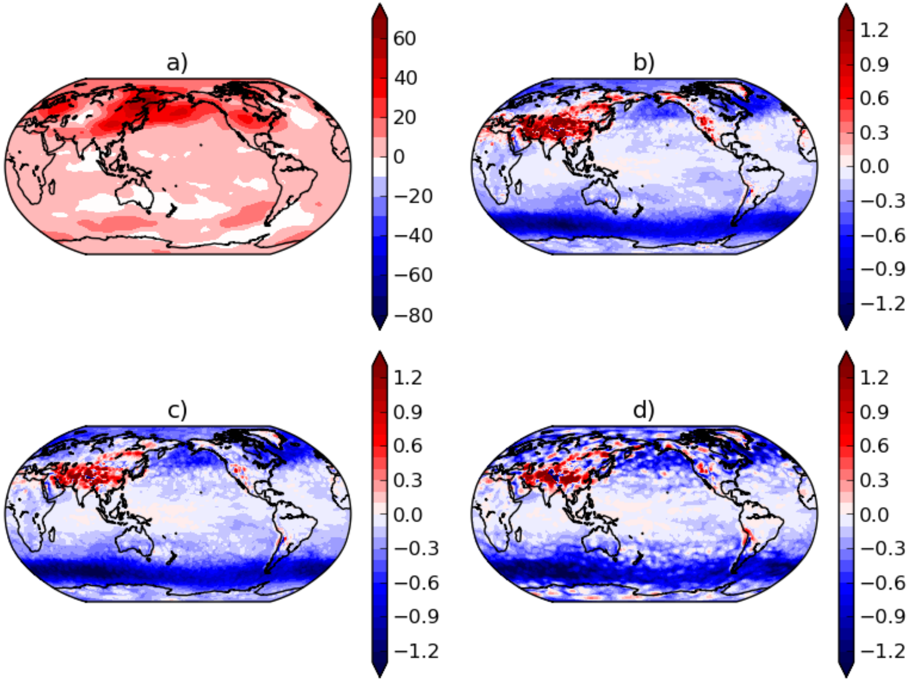

**Figure 2.** Spatial distributions of the difference in variance of air temperature between ACCESS simulations and ERAI. This is measured in Kelvin on a 2-D horizontal plane at 500 hPa and averaged over one year of simulation. **(a)** is the control with no nudging. **(b)** is the relaxation nudging hard nudging. **(c** and **d)** are spectral nudging using the 1-D filter with hard nudging, applied once an hour. Different nudging length scales were used: $\lambda = 0.1$ in **(c)** and $\lambda = 0.2$ in **(d)**. Note, for clarity, **(a)** uses a different scale for the contours.

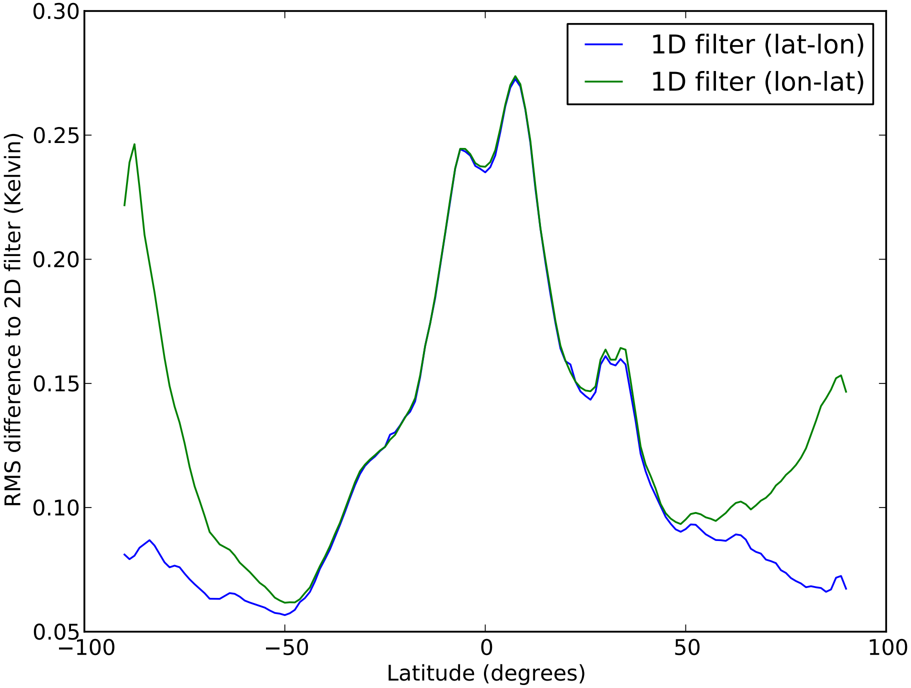

**Figure 3.** RMS difference, in air temperature at 500 hPa, of 1-D filters compared to the 2-D filter. Data was averaged temporally and zonally, for one year of data sampled every time-step. Each simulation uses the same nudging parameters, with hard nudging, using a filter length scale of $\lambda = 0.1$, applied once an hour.

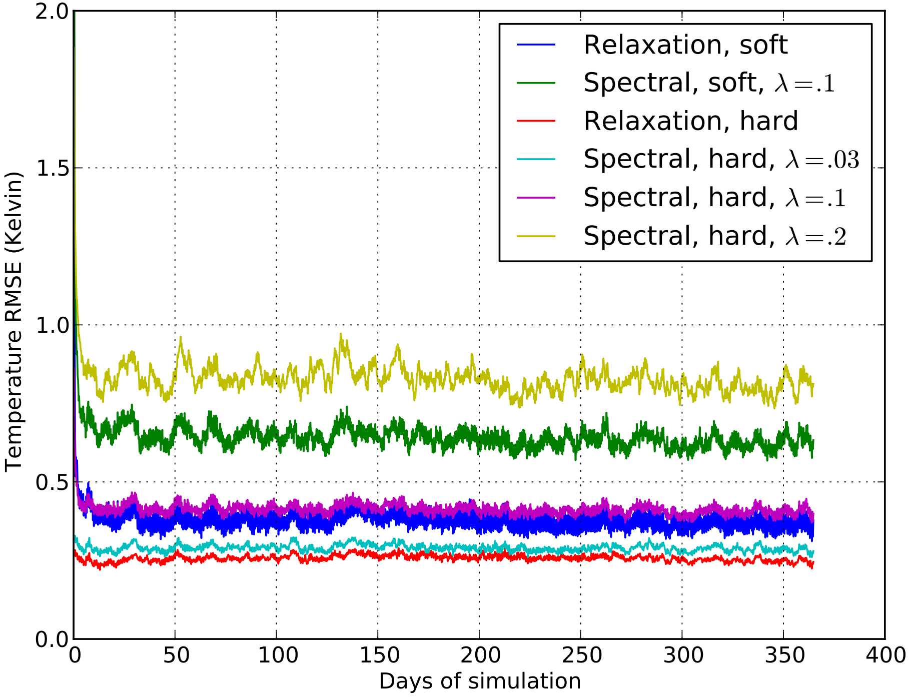

**Figure 4.** RMSE of temperature at 500 hPa, for a year of simulation. Simulations of relaxation and spectral nudging are compared, with strong or weak nudging, and several different spectral filter length scales. All of the spectral nudging simulations use the 1-D filter nudged once an hour.

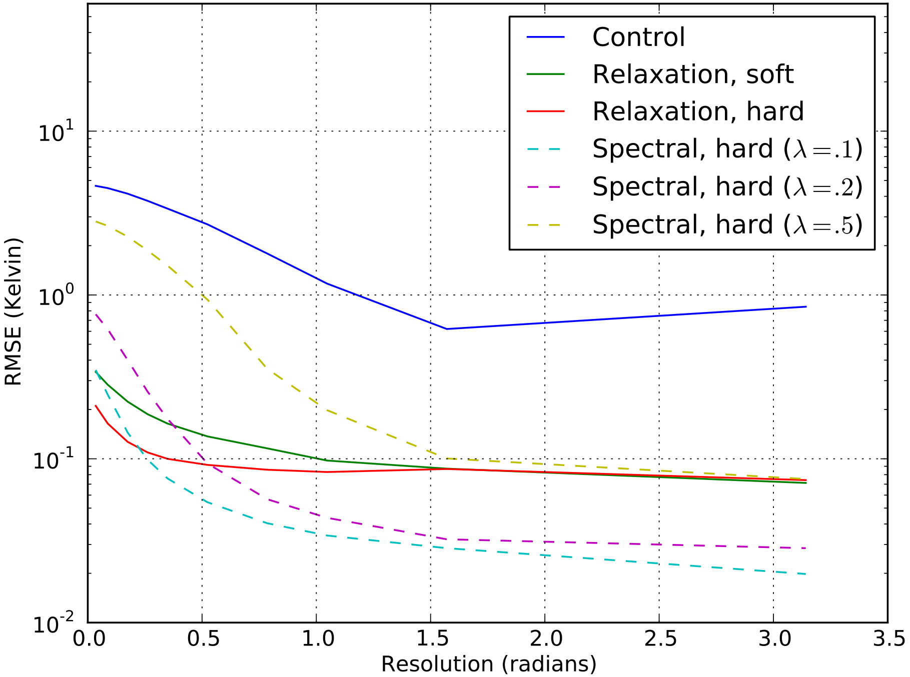

**Figure 5.** Plot of average RMSE of temperature at 500 hPa, at different regridded resolutions, for various simulations using nudging and a control simulation without nudging. All of the spectral nudging simulations use the 1-D filter nudged once an hour.

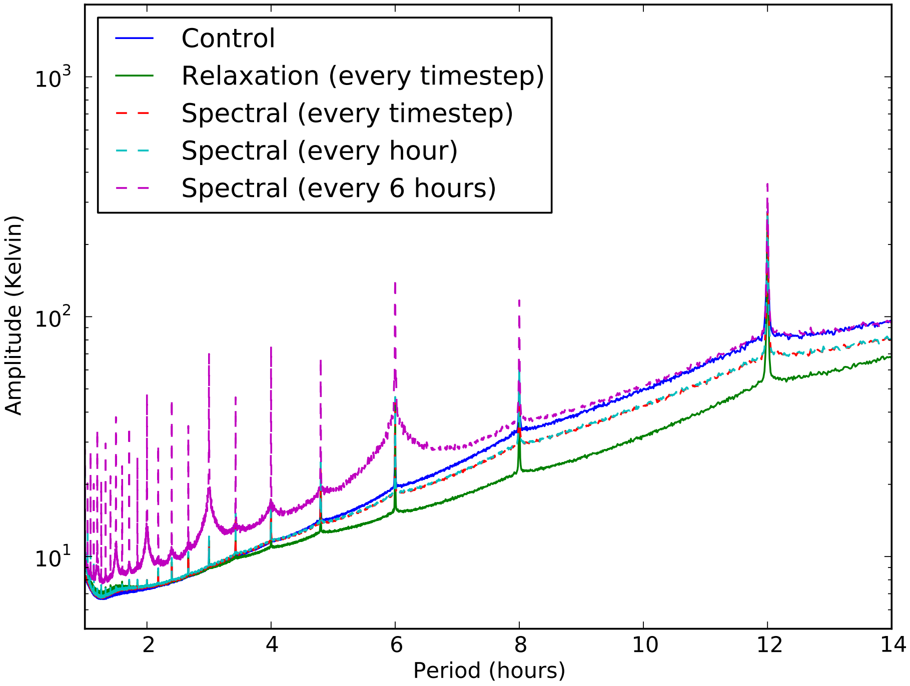

**Figure 6.** Temporal Fourier spectra for temperature at 500 hPa, for simulations with different nudging period. Soft nudging was applied and the spectral nudging simulations used a filter length scale of $\lambda = 0.1$.